X.L. DONG, J.W. WANG, Y.Q. CAI

ISSN 0543-5846
METABK 63(2) 257-260 (2024)
UDC – UDK 621.771:621.822:66.084:531.717:531.3-517.9=111

STUDY ON THE EFFECT OF WORK ROLL BEARING FIT CLEARANCE AND SPEED ON THE VIBRATION OF LEVELING MILL

Received – Primljeno: 2023-11-02
Accepted – Prihvaćeno: 2023-12-28
Original Scientific Paper – Izvorni znanstveni rad

The vibration of the leveling mill is common in metallurgical enterprises, which causes vibration marks on the surface of the support rolls and affects the surface quality of the strip. This paper establishes a bearing-rotor system model for a leveling mill, and finds that reducing the bearing clearance helps to improve the stability of the mill. The study of different speeds under the amplitude of the change, the work of the roll system gap changes on the vibration of the mill. Finally, the results of the study can provide reference for the theory of vibration suppression of rolling mills.

Keywords: rolling mill, roll bearing, vibration, leveling, dynamies equations

INTRODUCTION

Leveling mill vibration phenomenon is frequent [1] manifested as a new roll on the line after rolling a certain mileage support roll vibration mark phenomenon, forced to change the roll in advance, affecting the surface quality of the strip [2], reduce mill productivity [3-4]. Therefore, many experts and scholars in the mill vibration monitoring and theoretical exploration and other aspects of in-depth research, from the leveling mill intrinsic frequency and trigger factors to carry out research, resulting in the leveling mill vibration and intrinsic frequency similar to or overlap caused by vibration amplification. In this paper, based on the consideration of vertical structural support and bearing radial clearance, structural clearance change of work roll system and segmental nonlinear problem [5], the vertical nonlinear vibration model under the influence of elastic rolling force is established to provide reference for the study of mill vibration and related vibration suppression theory.

DYNAMIC MODELING OF AXIAL SEGMENTS

Considering the actual structure of the mill, a vertical vibration model of the structure shown in Figure 1 was developed. The shaft is discretized into 10 shaft segments, and the rolling force during the rolling process is applied to point 6. In addition, the rolling bearings are symmetrically distributed at node 3 and node 9, taking into account the nonlinear characteristics of the two bearings and the support when modeling the bearing dynamics. Each node is considered to have displacement degrees of freedom in the x-direction and y-direction, and the system has a total of 22 degrees of freedom.

Neglecting the influence of the corner, for the *i* th axial segmented unit, the node displacement can be expressed in a fixed coordinate system as follows:

$$\mathrm{u}_i(t) = \left[x_i(t), y_i(t), x_{i+1}(t), y_{i+1}(t)\right]^T \tag{1}$$

The differential equation of motion of the elastic shaft segment is:

$$(\mathbf{M}_T^e + \mathbf{J}_T^e)\ddot{u}^e(t) + \mathbf{K}_T^e u^e(t) = \mathbf{Q}^e \tag{2}$$

In Equation 2, $\mathbf{M}_T^e$ is the unitary mass matrix of the shaft segment, $\mathbf{J}_T^e$ is the unitary inertia matrix of the shaft segment, $\mathbf{K}_T^e$ is the unitary stiffness matrix of the shaft segment, and $\mathbf{Q}^e$ is the generalized force of the shaft segment.

$$\mathbf{M}_T^e = \frac{\rho A L_e}{840(1+\phi_e)^2}\begin{bmatrix} m_1 & m_2 & m_3 & m_4 \\ m_2 & m_5 & -m_4 & m_6 \\ m_3 & -m_4 & m_1 & -m_2 \\ m_4 & m_6 & -m_2 & m_5 \end{bmatrix} \tag{3}$$

$$\mathbf{J}_T^e = \frac{\rho I}{30(1+\phi_e)^2 L_e}\begin{bmatrix} m_7 & m_8 & -m_7 & m_8 \\ m_8 & m_9 & -m_8 & m_{10} \\ -m_7 & -m_8 & m_7 & m_8 \\ m_8 & m_{10} & -m_8 & m_9 \end{bmatrix} \tag{4}$$

$$\mathbf{K}_T^e = \frac{EI}{(1+\phi_e){L_e}^3}\begin{bmatrix} 12 & 6L_e & -12 & 6L_e \\ 6L_e & {L_e}^2(4+\phi_e) & -6L_e & {L_e}^2(2-\phi_e) \\ -12 & -6L & 12 & -6L_e \\ 6L_e & {L_e}^2(2-\phi_e) & -6L_e & {L_e}^2(4+\phi_e) \end{bmatrix} \tag{5}$$

X.L.Dong, J.W. Wang,Y.Q. Cai (E-mail: caiyq@ncst.edu.cn), College of Mechanical Engineering, North China University of Science and Technology, Hebei, Tangshan, China.

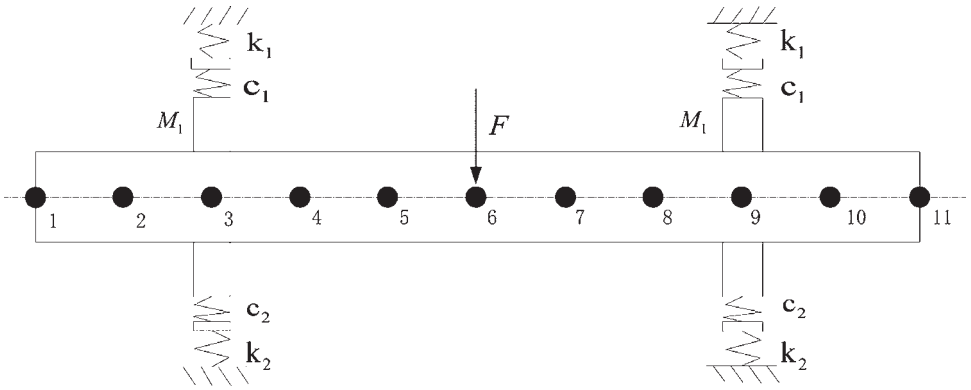

Figure 1 Physical modeling of the elastic shaft section of the work roll

Style:

$$\begin{aligned}
m_1 &= 312+588\phi_e+280\phi_e^{\,2}\\
m_2 &= (44+77\phi_e+35\phi_e^{\,2})L_e\\
m_3 &= 108+252\phi_e+140\phi_e^{\,2}\\
m_4 &= -(26+63\phi_e+35\phi_e^{\,2})L_e\\
m_5 &= (8+14\phi_e+7\phi_e^{\,2})L_e^{\,2}\\
m_6 &= -(6+14\phi_e+7\phi_e^{\,2})L_e^{\,2}\\
m_7 &= 36\\
m_8 &= (3-15\phi_e)L_e\\
m_9 &= (4+5\phi_e+10\phi_e^{\,2})L_e^{\,2}\\
m_{10} &= (-1-5\phi_e+5\phi_e^{\,2})L_e^{\,2}
\end{aligned} \tag{6}$$

Bearing theory model

The nonlinearities introduced into the rotor system by the radial clearance of the roller bearings are usually reduced to variable stiffness springs when analyzing the dynamic characteristics of the rotor system using finite elements.

Rolling bearing force is obtained according to the Hertz contact force formula, the rolling bearing is decomposed into the inner ring, outer ring and ball, assuming that the ball and the inner and outer ring for the pure rolling contact, as shown in Figure 2, and can be

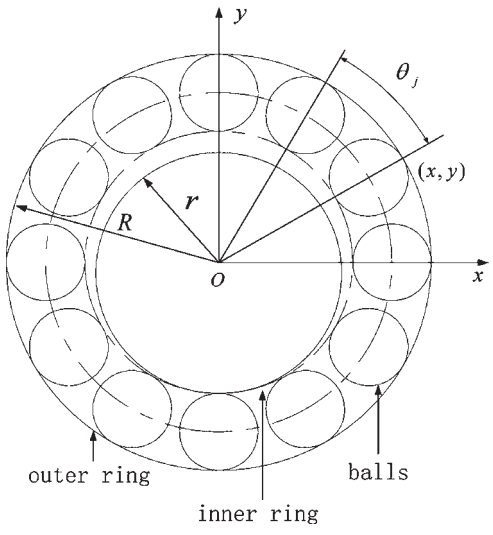

Figure 2 Bearing-rotor contact model

contacted and separated, the calculation is obtained to decompose the support force in the x and y directions as shown in the formula:

$$\begin{aligned}
Q_x &= K_c\sum_{j=1}^{N_b}(x\cos\theta_j+y\sin\theta_j-\lambda_0)^{10/9}\bullet\\
&\quad H(x\cos\theta_j+y\sin\theta_j-\lambda_0)\cos\theta_j\\
Q_y &= K_c\sum_{j=1}^{N_b}(x\cos\theta_j+y\sin\theta_j-\lambda_0)^{10/9}\\
&\quad \bullet H(x\cos\theta_j+y\sin\theta_j-\lambda_0)\sin\theta_j
\end{aligned} \tag{7}$$

where K_c is the contact stiffness coefficient and H is the H (•) function - Heaviside function as follows:

$$H(\theta_j)=\begin{cases}1, & \theta_j\geq 0\\ 0, & \theta_j<0\end{cases} \tag{8}$$

For bearings and bearing supports, the differential equations of motion are:

$$-\mathbf{C}\dot{u}(t)-\mathbf{K}_c u(t)=\mathbf{Q}^c \tag{9}$$

SYSTEM DYNAMICS MODEL

By assembling the matrix of each unit of the rotor shaft, the total finite element assembly matrix of the rotor shaft can be obtained. In the assembly process, the left node degree of freedom of the unit is connected to the right node degree of freedom of the neighboring unit on the left, and then the right node degree of freedom of the unit is connected to the left node degree of freedom of the neighboring unit on the right, and at the position where the left and right nodes are connected. $\mathbf{M}_T^e$, $\mathbf{J}_T^e$ and $\mathbf{K}_T^e$ are combined in the above manner, and after combination, they are composed in the form of diagonal arrays.

By using Eq. 2 and Eq. 9, the differential equation of the dynamics of the bearing-rotor system can be obtained as:

$$(\mathbf{M}_T+\mathbf{J}_T)\ddot{u}(t)-\mathbf{C}\dot{u}(t)+(\mathbf{K}_T-\mathbf{K}_c)u(t)+\mathbf{Q}(t)=F \tag{10}$$

Nonlinear vibration analysis

The radial clearance of the bearing causes localized shock phenomena in the bearing-rotor system, which is one of the important sources of nonlinear vibration in

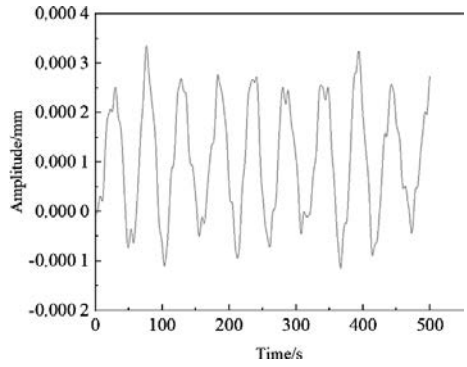

Figure 3 X-direction time-domain plot 0,05 mm

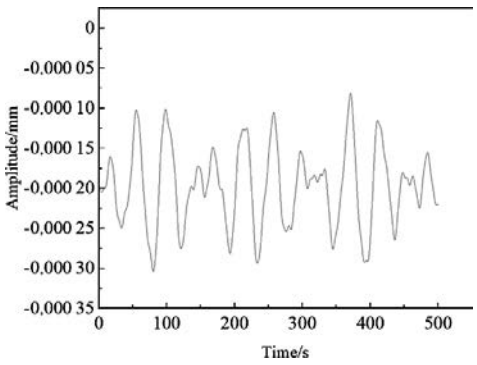

Figure 4 Y-direction time-domain plot 0,05 mm

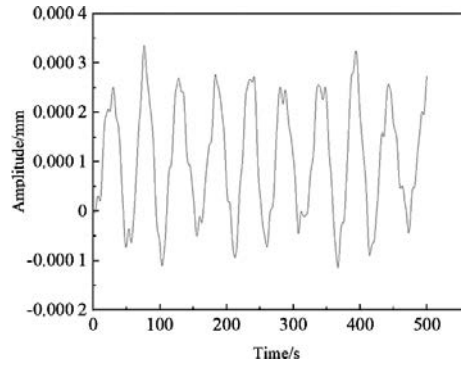

Figure 5 X-direction time-domain map 0,1 mm

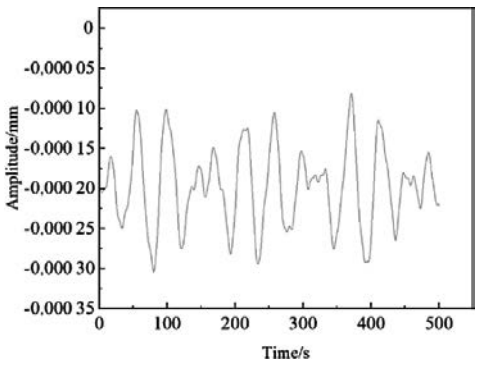

Figure 6 Y-direction time-domain map 0,1 mm

the rotor system, and the radial clearance (0,05 mm, 0,1 mm) of the rolling bearing is investigated. The fourth-order Runge-Kutta method is used to solve the system numerically and obtain the time-domain response of the system. The time domain plots of the rotor system at node 6 are shown in Figures 3 to 6 for different rolling bearing radial clearances in the x and y directions, respectively.

It can be seen from the above Figure: as the radial clearance of the bearing increases from 0,05mm to 0,1mm, the amplitude of the vibration signal also increases. When the clearance increases, there are obvious localized shocks and vibration fluctuations in the time domain waveform, which is due to the existence of radial clearance and thus reduces the support stiffness of the bearing, resulting in radial collision of the system.

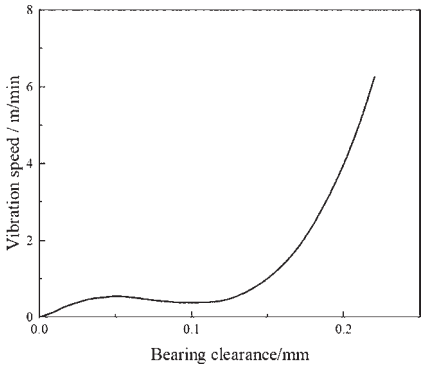

Figure 7 Relationship between fit clearance and vibration speed of 2 m/min

As can be seen in Figure 7, when the gap reaches 0,15mm, the vibration amplitude rises sharply. Through simulation, it can be seen that the larger the gap, the larger the vibration of the work roll, and the gap plays a role in amplifying the vibration.

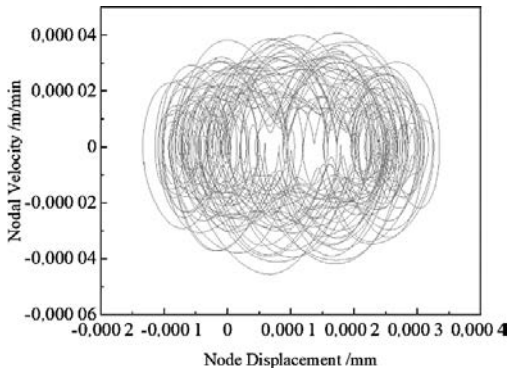

Figure 8 Phase diagram of the axial trajectory at a speed of 2 m/min

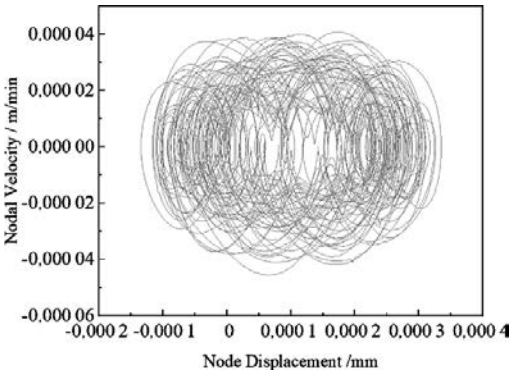

Figure 9 Phase diagram of the axial trajectory at a speed of 7 m/min

In order to investigate the effect of input speed on the vibration of the system, five different input speeds (2 m/min, 7 m/min) are considered while keeping other factors constant. Figure 8 and Figure 9 show the variation rule of the axial trajectory at different speeds, respectively.

Increasing the working roll speed increases its centrifugal force. When the working roller speed is increased from 2 m/min to 7 m/min, it is obvious that the vibration amplitude of the system decreases.

CONCLUSION

By establishing a nonlinear vibration model of the bearing-rotor system, two conclusions can be drawn:

(1) It is found that as the radial clearance of the bearing decreases, the vibration of the rolling mill system is smaller.

(2) It is found that as the speed of the work roll system changes differently, the vibration system shows a stabilizing trend.

Therefore, the appropriate reduction of the gap between the work roll structure and the increase in speed will help to improve the stability of the system. The results of the study can provide relevant theoretical references for the mill structure and vibration nonlinear problems.

REFERENCES

[1] Runlin C, Jiaxin L, Jie T, et al. Vibration characteristics analysis of rolling bearing rotor system considering radial clearance and outer raceway defect [J]. Advances in Mechanical Engineering, 15 (2023)4.

[2] Rongrong P . Nonlinear vibration characteristics and time-delayed displacement control of rolling mill under dynamic rolling force [J]. Journal of Vibroengineering, 23 (2021)7.

[3] Rongrong P, Xingzhong Z, Peiming S. Vibration Characteristics of Hot Rolling Mill Rolls Based on Elastoplastic Hysteretic Deformation [J]. Metals,11(2021)6.

[4] Hou D, Xu L, Shi P. Vertical–horizontal coupling nonlinear vibration characteristics of rolling mill under mixed lubrication [J]. Journal of Iron and Steel Research International, 28(2021)5.

[5] Sun P Y, Zhang C D. Research on the Vibration of Rolling Mill [J]. Advanced Engineering Forum, (2011)2-3,1598.

Note: The responsible translator for English language is Q.Q. Yin -NCST.